Eastern Michigan University
DigitalCommons@EMU

Master's Theses and Doctoral Dissertations

Master's Theses, and Doctoral Dissertations, and Graduate Capstone Projects

2011

Characterizing the oligomeric structure and catalytic activity of the dihydroorotase and aspartate transcarbamoylase from the bacterium, *bacillus anthracis*

Reshma Kankanala

Follow this and additional works at: http://commons.emich.edu/theses

 Part of the Chemistry Commons

Recommended Citation
Kankanala, Reshma, "Characterizing the oligomeric structure and catalytic activity of the dihydroorotase and aspartate transcarbamoylase from the bacterium, *bacillus anthracis*" (2011). *Master's Theses and Doctoral Dissertations*. 339.
http://commons.emich.edu/theses/339

This Open Access Thesis is brought to you for free and open access by the Master's Theses, and Doctoral Dissertations, and Graduate Capstone Projects at DigitalCommons@EMU. It has been accepted for inclusion in Master's Theses and Doctoral Dissertations by an authorized administrator of DigitalCommons@EMU. For more information, please contact lib-ir@emich.edu.

Characterizing the oligomeric Structure and Catalytic Activity of the Dihydroorotase and Aspartate Transcarbamoylase from the Bacterium, *Bacillus anthracis*

by

Reshma Kankanala

Thesis

Submitted to the Department of Chemistry

Eastern Michigan University

in partial fulfillment of requirements

for the degree of

MASTER OF SCIENCE

in

Chemistry

August 2011

Ypsilanti, Michigan.

Dedication

to

Chemistry Department, EMU.

Acknowledgements

I would like to express my sincere gratitude to my research advisor, Dr. Hedeel Evans. Thanks for giving me the opportunity to be a part of this research. It has been an honor to work with her. Her interest, knowledge, time, patience, and understanding helped me in the successful completion of this project.

Besides my advisor, I would like to thank my thesis committee members, Dr. Steven Pernecky and Dr. Deborah Heyl-Clegg, for agreeing to be on the committee. Their encouragement, insightful comments, and hard questions helped me a lot in this research.

I would like to thank my graduate advisor, Dr. Timothy Brewer, for his excellent support by awarding me a graduate assistantship and for his valuable academic suggestions throughout my Master's studies in the chemistry department.

I would like to thank the head of the chemistry department, Dr. Ross Nord, all the professors, staff, and all my friends at the EMU chemistry department, who helped me during my Masters at Eastern Michigan University.

Finally, I would like to thank my parents for their moral support throughout my Master's degree program at Eastern Michigan University.

Abstract

Bacteremia refers to bacterial presence in the blood. Bacterial proliferation in the blood requires that the organism adapt its metabolism to available nutrients. Nucleotide precursors that could be used are present at low levels in the blood, and thus the invading bacteria must rely on *de novo* nucleotide biosynthesis for survival. The dihydroorotase domain is a key enzyme in pyrimidine biosynthesis and a promising drug target. The genes encoding the dihydroorotase (DHOase) and aspartate transcarbamoylase (ATCase) of *Bacillus anthracis* (*B. anthracis*) were cloned for expression in *Escherichia coli* (*E. coli*). The proteins were purified by affinity chromatography and the enzymatic activity was determined by enzyme assays. The data suggests that a physical and functional interaction exists. The activity of ATCase was increased by about 2 fold in the presence of an equimolar concentration of DHOase. An ATCase-DHOase complex was formed as judged by S-300 gel filtration chromatography and cross-linking methods. Moreover, orotate was found to be an effective inhibitor of the DHOase activity at nanomolar concentrations. These results bring us closer to understanding the structural organization of the pyrimidine pathway in the pathogenic *B. anthracis* bacterium and provide a lead in the design of drugs selective to the bacteria.

Table of Contents

List of Figures

1. Introduction

1.1 Bacteremia

The presence of bacteria in the bloodstream is referred to as bacteremia, a major cause of morbidity and mortality worldwide.[1, 2] The growth of bacterial pathogens in the blood represents one of the most dangerous stages of infection. The *B. anthracis* infection is characterized by the rapid growth of the bacteria in the host's blood, reaching up to10^8 bacteria/ml.[3] Bacteremia often leads to severe illness and death.

While growing in the blood, bacteria do not only attempt to evade the immune response of the host, but also adjust their metabolism to suit the availability of nutrients. For the proliferation of bacterial pathogens in human blood, bacteria need to synthesize metabolites that are present in limiting concentrations. For that, they need to produce specific enzymes that are critical for the growth of the bacteria in the bloodstream. Certain nutrients are scarce in the blood and need to be synthesized *de novo* by the proliferating bacteria in the blood. *E. coli* is a major cause of Gram-negative bacteremia in hospitalized patients. A recent comprehensive, genome-wide search [4] for genes that are essential for growth in human serum showed that a majority of the mutants identified consistently carried a deletion of a gene involved in either the purine or pyrimidine nucleotide biosynthetic pathway.

The limited supply of nucleotide precursors appears to be the key limitation for bacterial growth in serum. Inactivation of genes involved in nucleotide biosynthesis led to significant growth defects in human serum not only for *E. coli* but also for *Salmonella Typhimurium* and *B. anthracis*. The study clearly shows that *de novo* nucleotide biosynthesis represents the single most critical metabolic need for bacterial growth in blood and is likely to be the only metabolic pathway that is indispensible for bacterial pathogens invading the blood. The corresponding enzymes involved in nucleotide biosynthesis are thus promising antibiotic targets for reducing bacterial growth and the treatment of bloodstream infections.

More specifically, of the enzymes identified to be

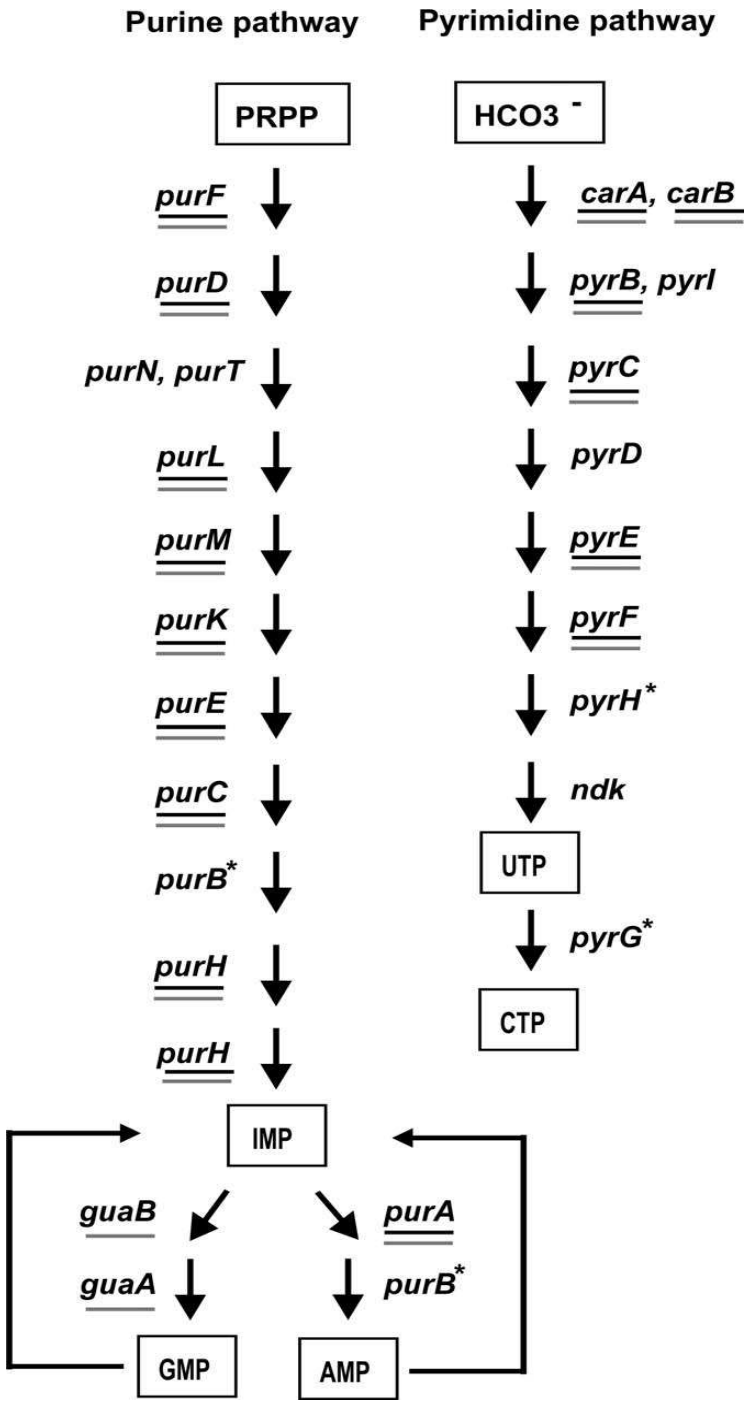

Figure 1: Genes involved in the purine and pyrimidine biosynthetic pathways.

essential for growth of pathogenic bacteria in human blood, two, PyrC and PurE, are especially attractive as targets for antibiotics. PyrC encodes dihydroorotase that catalyzes the reversible cyclization of carbamoyl aspartate to dihydroorotate in the third step of the pyrimidine biosynthesis pathway [5] (Figure 1).

A detailed examination of PyrC and PurE gene products, as well as other enzymes of the nucleotide biosynthesis pathways, as potential antibiotic targets may ultimately lead to the development of new therapies for treatment of bacterial bloodstream infections.

1.2 Anthrax

Anthrax is a life-threatening infectious disease that is very often lethal.[6] It can affect animals and humans and is caused by the bacterium *Bacillus anthracis*. Anthrax does not spread from person to person. However, the disease can spread from diseased animals to humans by directly contacting the diseased animal or by food consumption of the infected animals. Anthrax is spread by spores, such as via air inhalation, but does not spread directly from an infected animal or person to another.

Anthrax organisms in the soil are dormant in the form of endospores or spores, which are difficult to destroy and able to survive in harsh and extreme conditions for a long period of time lasting as long as 48 years.

Spores may reactivate and multiply rapidly upon inhalation, ingestion, or contact of spores with skin lesions on the host. If anthrax spores are inhaled, they can

migrate and proliferate in the lymph glands in the chest area, leading to them spreading within the body. Death is often the end result due to toxin production.

More recently, anthrax has received a lot of attention as its spores can be produced *in vitro* and used as a biological weapon. Funding is available for anthrax research as the U.S. government largely lacks the range of medical countermeasures needed to protect citizens from anthrax and other potential bioweapons.

Anthrax causes three forms of disease: cutaneous anthrax, inhalation anthrax, and gastrointestinal (bowel) anthrax.

1.2.1 Cutaneous (skin) anthrax: This form of anthrax most commonly results when humans handle the products of diseased animals. It normally begins as a reddish spot that becomes enlarged and hardened. Lymph glands present in the area may become swollen. Symptoms can include muscle aches, pain, fever, and headaches. This form of anthrax is typically resolved in about six to seven weeks.

1.2.2 Inhalation anthrax: The first symptoms are subtle, gradual, and flu-like and may develop in one to six days. These may include sore throat, fever, and muscle pain. However, in a few days, the illness worsens and may result in severe respiratory distress. Shock, coma, and death may follow. Even upon aggressive treatment, once severe symptoms develop, 45% to 80% of patients typically die, and if left completely untreated, the death rate can exceed 99%.

1.2.3 Gastrointestinal anthrax: This form is rare. It is caused by consumption of infected, contaminated, or undercooked meat. The symptoms include nausea, bloody

diarrhea, loss of appetite, fever, and abdominal pain. Once the anthrax bacteria invade the bowel wall, septicemia may result, where the infection spreads via the bloodstream throughout the body with deadly toxicity.

1.2.4 Antibiotic therapy: Currently existing drugs are mainly effective if treatment is started early enough. Common antibiotics such as penicillin, tetracycline, and ciprofloxacin, are used to treat the cutaneous form of anthrax. Antibiotics delivered early via intravenous therapy are typically employed continuously for the pulmonary inhalation form.

1.3 Bacillus Anthracis (*B. anthracis*)

B. anthracis is a spore-forming bacterium that can be grown under aerobic or anaerobic conditions. It is a Gram-positive, rod-shaped bacterium that is about 1-1.2μm wide and 3-5μm long. It is the only bacterium, thus far, known to synthesize a protein capsule. The spores of the bacteria are highly resilient and can survive and withstand low nutrient environments and extremes of temperatures for centuries.

1.4 The Pyrimidine Biosynthetic Pathway

Pyrimidine nucleotides play a critical role in cellular metabolism. They serve as activated precursors of RNA and DNA, CDP-diacylglycerol phosphoglyceride for the assembly of cell membranes, and UDP-sugars for protein glycosylation and glycogen synthesis. There are two routes to the synthesis of pyrimidines; nucleotides can be recycled by the salvage pathways or synthesized *de novo* from small metabolites.

Most cells have several specialized passive and active transporters that allow the reutilization of preformed pyrimidine nucleosides and bases.

The *de novo* pyrimidine biosynthetic pathway (Figure 2) is indispensable in proliferating cells in order to meet the increased demand for nucleic acid precursors and other cellular components. Pyrimidine biosynthesis is invariably up-regulated in tumors and neoplastic cells and has been linked to the etiology or treatment of several other disorders including AIDS, diabetes, and autoimmune diseases, such as rheumatoid arthritis.

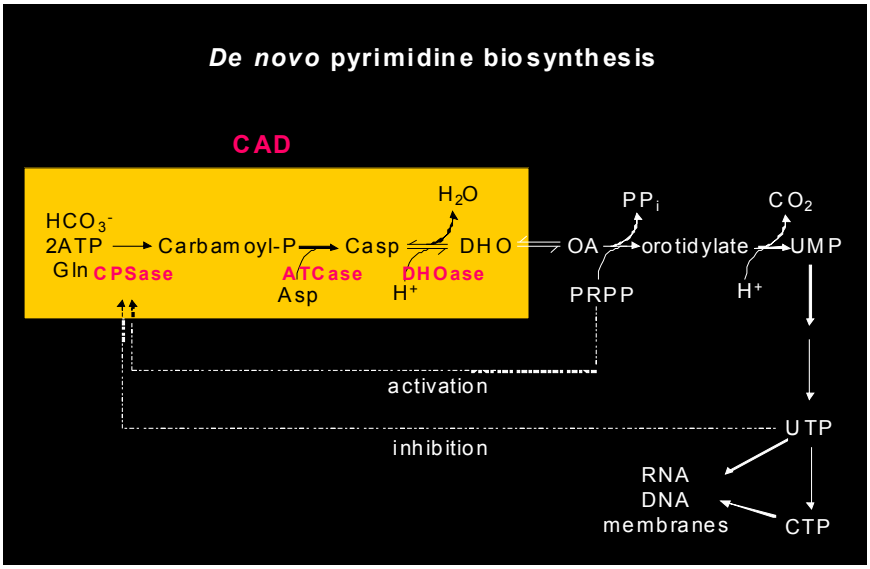

Figure 2: The *de novo* pyrimidine biosynthesis pathway.

1.4.1 Aspartate Transcarbamoylase (ATCase): ATCase catalyzes the reaction of carbamoyl phosphate and aspartate to form carbamoyl aspartate (Figure 2). In mammalian cells, CAD is a multifunctional protein that catalyzes the first three steps of the pyrimidine biosynthetic pathway. The carbamoyl phosphate synthetase (CPSase) domain catalyzes the first step in the pathway. The ATCase domain is unregulated and catalyzes the second step in the pathway. The isolated CAD ATCase domain is a homotrimer of 34-kDa subunits.[7] Kinetic and modeling studies showed that the mammalian domain shares a common catalytic mechanism, oligomeric structure, and

tertiary-fold with the *E. coli* ATCase catalytic subunit, [8-11] including a composite active site comprised of residues from adjacent subunits. The trimeric ATCase interactions are a crucial organizing element in the CAD hexamer.

1.4.2 Dihydroorotase (DHOase): The DHOase domain catalyzes the third step in the pathway, the reversible condensation of carbamoyl aspartate to dihydroorotate (Figure 2). It is a zinc metalloenzyme. The active site of *E. coli* DHOase has two zinc ions and a carboxylysine that bridges the metal centers.[12] DHOases are classified [13] into two major classes. Type I DHOases are the most ancient and include domains of multifunctional proteins, such as CAD, subunits of multienzyme complexes, and monofunctional enzymes. The type II enzymes, such as *E. coli* DHOase, are a more recent evolutionary development and are smaller in size. The isolated CAD DHOase domain has only one zinc atom and is larger than its bacterial counterpart, consistent with its assignment as a type I DHOase.[14-17] The forward DHOase reaction is favored at low pH (below pH 6), and the reverse reaction is favored at high pH (above pH 8).

1.5 *B. anthracis* DHOase

The isolated DHOase from *B. anthracis* is a homodimer.[18] The secondary structure of two chains is identical, with two zinc atoms in each chain and a total of 180 water molecules. An overall tertiary structure is formed from the TIM-barrel secondary structure motif.

The active site of the enzyme includes a binuclear Zn center.[18] His59, His61, Asp151, and Asp304 are bound to the more buried α Zn atom while His178, His231, and Asp151 bind to the β Zn atom. Asp151, via its carboxylate side group, forms a bridge between the two Zinc atoms, separated by 3.3 Å. There is a large interface in the structure between the monomers, which involves 18 residues from one chain and 17 residues from the other (Figure 3).

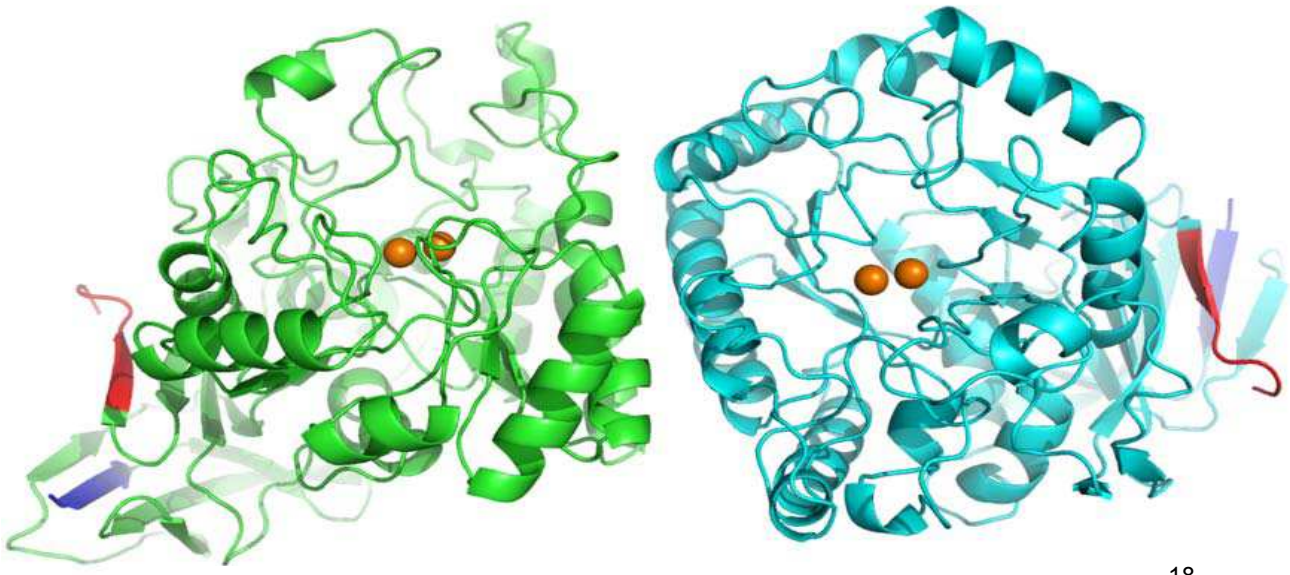

Figure 3: Homodimer of the dihydroorotase from *B. anthracis* at 2.6 Å resolution[18]

1.6 *Aquifex Aeolicus (A. aeolicus)*

A. aeolicus is a rod-shaped hyperthermophilic bacterium of ancient lineage. It grows best in water between 85-95 ºC. It is found near volcanoes and hot springs. The genome of *A. aeolicus* is only about a third of that of *E. coli.*

1.7 Sequence homology of *B. anthracis* and *A. aeolicus* DHOase

The DHOase from *B. anthracis* is highly conserved in sequence to that of *A. aeolicus.* The percent sequence identity is 43% (Figure 4).

Score = 321 bits (822), Expect = 3e-89, Method: Compositional matrix adjust.
Identities = 182/426 (43%), Positives = 257/426 (61%), Gaps = 10/426 (2%)

```
B. an  1    MNYLFKNGRYM----NEEGKIVATDLLVQDGKIAKVAENITADNAEVIDVNGKLIAPGLV  56
            +  + KNG  +    N EG+    D+LV++GKI K+ +NI    AE+ID  G ++ PG +
A. ae  2    LKLIVKNGYVIDPSQNLEGEF---DILVENGKIKKIDKNILVPEAEIIDAKGLIVCPGFI  58

B. an  57   DVHVHLREPGGEHKETIETGTLAAAKGGFTTICAMPNTRPVPDCREHMEDLQNRIKEKAH  116
            D+HVHLR+PG  +KE IE+G+  A  GGFTTI  MPNT P  D    +  +  + K
A. ae  59   DIHVHLRDPGQTYKEDIESGSRCAVAGGFTTIVCMPNTNPPIDNTTVVNYILQKSKSVGL  118

B. an  117  VNVLPYGAITVRQAGSEMTDFETLKELGAFAFTDDGVGVQDASMMLAAMKRAAKLNMAVV  176
              VLP G IT  + G E+ DF +LKE G  AFTDDG  V D+S+M  A++ A++L + ++
A. ae  119  CRVLPTGTITKGRKGKEIADFYSLKEAGCVAFTDDGSPVMDSSVMRKALELASQLGVPIM  178

B. an  177  AHCEENTLINKGCVHEGKFSEKHGLNGIPSVCESVHIARDILLAEAADCHYHVCHVSTKG  236
             HCE++ L   G ++EG+ S   GL+      E + IARD +LA+    H H+ HVSTK
A. ae  179  DHCEDDKL-AYGVINEGEVSALLGLSSRAPEAEEIQIARDGILAQRTGGHVHIQHVSTKL  237

B. an  237  SVRVIRDAKRAGIKVTAEVTPHHLVLCEDDIPSADPNFKMNPPLRGKEDHEALIEGLLDG  296
            S+ +I   K  G+K+T EV P+HL+  E ++ ++  N ++NPPLR KED  ALIEG+  G
A. ae  238  SLEIIEFFKEKGVKITCEVNPNHLLFTEREVLNSGANARVNPPLRKKEDRLALIEGVKRG  297

B. an  297  TIDMIATDHAPHTAEEKAQGIERAPFGITGFETAFPLLYTNLVKKGIITLEQLIQFLTEK  356
             ID  ATDHAPH   EK + +E A  GI G +TA P     L +KGII+L++LI+  T
A. ae  298  IIDCFATDHAPHQTFEK-ELVEFAMPGIIGLQTALPSAL-ELYRKGIISLKKLIEMFTIN  355

B. an  357  PADTFGLEAGRLKEGRTADITIIDLEQEEEIDPTTFLSKGKNTPFAGWKCQGWPVMTIVG  416
            PA   G++ G LK G  ADITI D  +E  ++  T LSK +NTP  G   +G  + TI
A. ae  356  PARIIGVDLGTLKLGSPADITIFDPNKEWILNEETNLSKSRNTPLWGKVLKGKVIYTIKD  415

B. an  417  GKIAWQ  422
            GK+ ++
A. ae  416  GKMVYK  421
```

Figure 4: Sequence homology of B. Anthracis and A.aeolicus DHOase

1.8 DHOase from *A. aeolicus*

Unlike the DHOase from *E. coli* and *B. anthracis*, the DHOase from *A. aeolicus* has a single zinc ion (Figure 5) present only in the α site. Moreover, the structure has three disordered surface loops near the active site and a complete composite domain involving both N-terminal and C-terminal segments.[19]

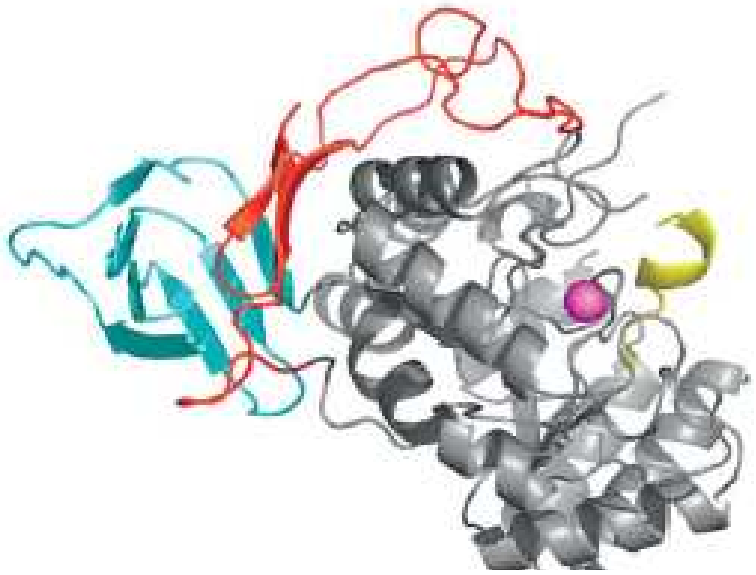

Figure 5: Three-dimensional structure and active site of *A. aeolicus* DHOase

The isolated *A. aeolicus* DHOase domain is catalytically inactive (Figure 5) despite the presence of the zinc and all of the active site residues needed for catalysis. That activity is completely regained, however, upon association with *A. aeolicus* ATCase. A 1:1 stoichiometric complex of *A. aeolicus* DHOase and ATCase can be reconstituted and is fully active.[19]

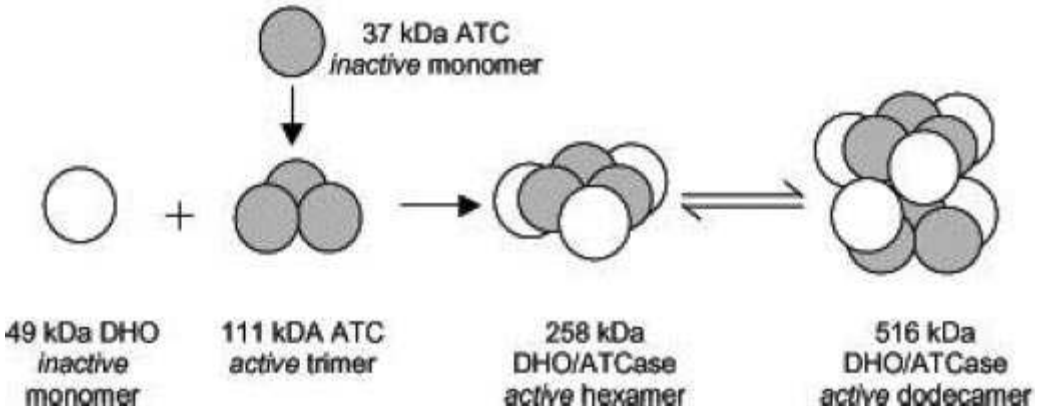

Figure 6: Model for the assembly of the *A. aeolicus* DHOase-ATCase complex.

Both the DHOase and ATCase monomers are inactive. A mode for the complex formation may be that the ATCase associates form a catalytically active trimer, which then associates with the DHOase monomers to form a hexamer that has both DHOase and ATCase activities (Figure 6).

The 1:1 stoichiometric complex was found to exist as an equilibrium mixture of $(ATCase)_3(DHOase)_3$ hexamers and $((ATC)_3(DHOase)_3)_2$ dodecamers.[19] Significantly, the DHOase component, as well as the ATCase, in the complex is catalytically active.

Interestingly, while the DHOase appears to rely on the ATCase for its catalytic activity, the converse does not appear to be true as the *A. aeolicus* ATCase is not activated by DHOase.

1.9 A stoichiometric complex (DAC) of *A. aeolicus* DHOase and ATCase

A stoichiometric complex of *A. aeolicus* DHOase forms with ATCase in a hollow, hetero-dodecamer (Figure 7), in which all 12 enzyme active sites face an aqueous cavity with limited access to the exterior. This amazing architecture may facilitate allosteric communication between the active sites and possibly increases the net production of dihydroorotate, which is thermodynamically unfavored at physiological pH.

The three active site loops that are intrinsically disordered in the free, inactive DHOase, described above, are ordered in the DAC complex.

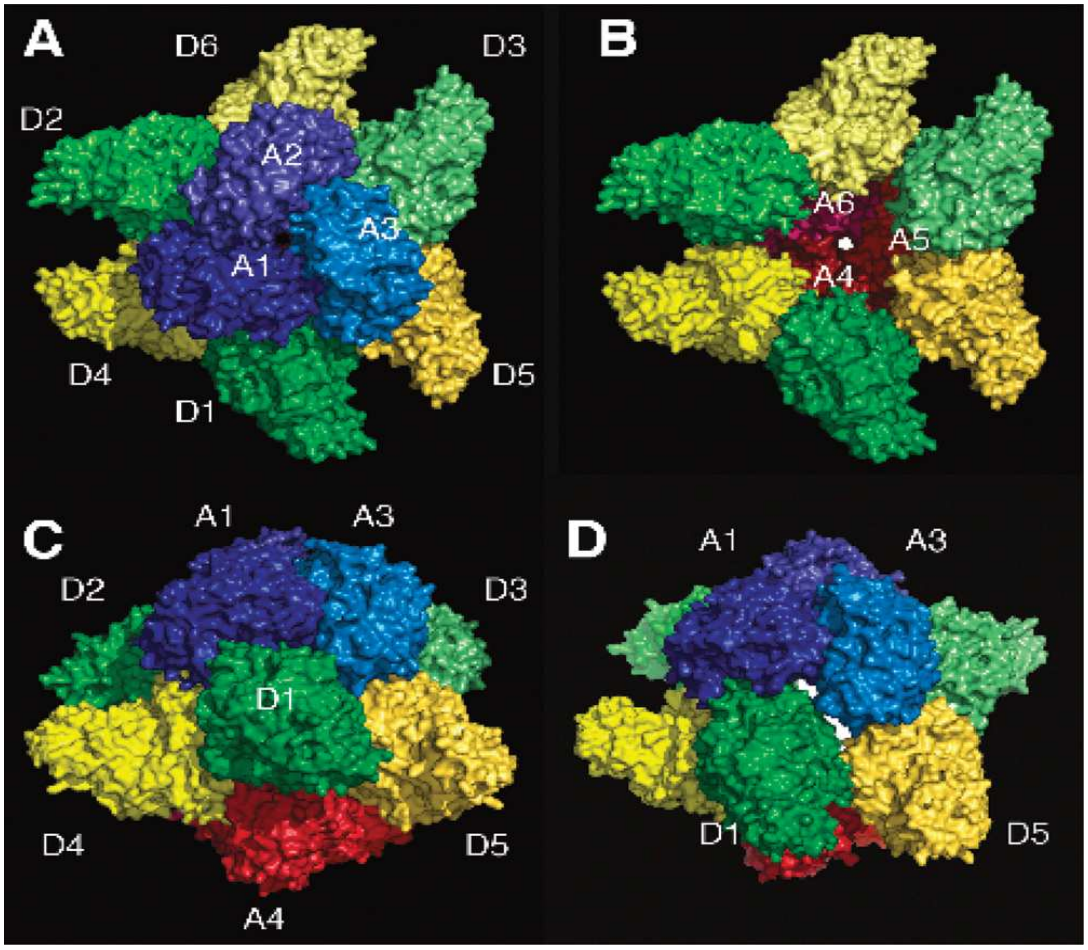

Figure 7: The DAC dodecamer

2. Research Goal and Objectives

The overall goal of this research work is to more thoroughly characterize the second and third steps in *de novo* pyrimidine biosynthesis in *B. anthracis* and to gain a better understanding of the structural and functional organization of the *B. anthracis* ATCase and DHOase domains.

2.1 Significance of the Proposed Study

The DHOase has recently emerged as a promising drug target that may ultimately lead to new therapies and pave the way for structure-based drug discovery for treatment of Anthrax and other bacterial bloodstream infections.

2.2 Hypothesis

Anthrax ATCase and DHOase physically interact to form a dodecamer that resembles that of *A. aeolicus* in structure and function.

2.3 Specific aims/goals

1) Identify whether the *B. anthracis* DHOase and ATCase form a physical complex. This can be investigated by cross-linking and by determining the oligomeric structure of the individual proteins and their mixtures by gel filtration chromatography. The fractions can be collected from the column and analyzed by SDS-PAGE. Enzyme activities will be determined by enzyme assays.

2) Explore the putative functional interactions of ATCase and DHOase. The proteins will be mixed in different stoichiometric ratios and their activities measured by the corresponding enzyme assays.

3) Study the effect of inhibitors previously used for the mammalian system, such as Orotate, 5-amino-orotic acid, and 5-fluoro-orotic acid. Enzyme assays will be carried out in the presence and absence of inhibitors.

3. Methods and Materials

3.1 Materials

Reagents including aspartate, carbamoyl aspartate, dihydroorotate, antipyrine, diacetyl monoxime, carbamoyl phosphate used for enzyme assays, High Resolution Sephacryl S-300 used for gel filtration chromatography, and the antibiotic ampicillin, were all purchased from Sigma-Aldrich. The bacterial strain, BL21 (DE3), used for expression of recombinant proteins and the bench mark prestained protein ladder, were from Invitrogen.

3.2 Expression and Isolation of the Recombinant Proteins

Plasmid DNA encoding *B. anthracis* ATCase and DHOase were transformed separately into the *E. coli* strain BL21 (DE3). The transformants were grown on agar plates containing ampicillin. A single colony was selected and grown at 37 °C in an overnight 15-ml culture consisting of LB medium and 100 µg/ml ampicillin. The overnight culture was then inoculated into a 125-ml LB medium containing 100 µg/ml of ampicillin and grown at 37^{o}C. The cells were harvested and the pellet was resuspended in 3 ml of 50 mM Tris/HCl, pH 8. The cells were disrupted by sonication for 30 s in an ice/water bath for a total of five times with five minutes intervals to prevent overheating. The cell extract was centrifuged at 14,000 rpm for 30 min at 4 °C, and the supernatant from the centrifuged fractions was collected and loaded onto a 1-ml Ni^{2+}-ProBond column equilibrated with 20 ml of 50 mM Tris/HCl, pH 8, 200 mM NaCl (TN buffer). The *B. anthracis* ATCase and DHOase were eluted with

successive 3-ml aliquots of increasing concentrations of imidazole up to 300 mM in TN buffer. The fractions were collected and analyzed by electrophoresis on 12% SDS-PAGE gels and by enzyme activity assays.

3.3 ATCase Assay

The ATCase activity was determined by measuring the time dependent formation of carbamoyl aspartate from carbamoyl phosphate and aspartate.

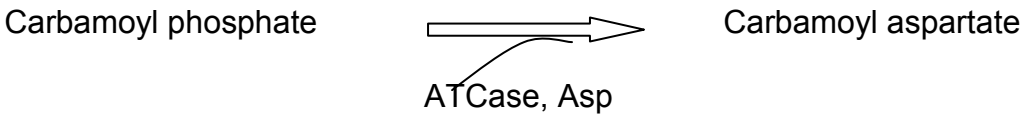

The assay mixture consisted of 2 mM aspartate, 50 mM Tris/acetate buffer, pH 8.3, and 2-3 µg of purified ATCase in a total volume of 1 ml. Samples were allowed to preincubate at 37°C for 20 min. The reaction was then initiated by the addition of 100µl of 50 mM carbamoyl phosphate at 37^{o}C and allowed to proceed for 10 min. The reaction was then quenched with 1 ml of 5% acetic acid. A 2ml color mix which contains antipyrine/diacetyl monoxime was added to generate a yellow color and the assay mixture was heated at 60°C for 30-90 min for color development. The carbamoyl aspartate generated by ATCase is converted into a yellow- colored compound, and the absorbance was measured at 466 nm on a spectrophotometer.

3.4 DHOase Assay

The DHOase assay measured the reverse reaction, formation of carbamoyl aspartate from dihydroorotate, as the equilibrium strongly favors dihydroorotate hydrolysis under

the assay conditions. The formation of carbamoyl aspartate was quantitated at 466 nm, as described above.

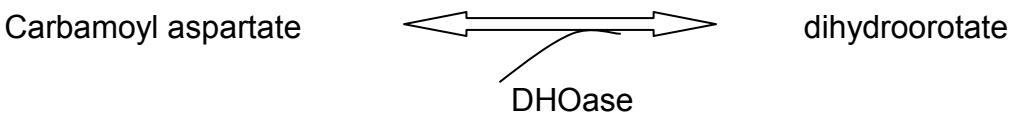

The assay mixture consisted of 2-3 µg of purified DHOase, 50 mM Tris/acetate, pH 8.3, and 10% glycerol, in a total volume of 1ml. The tubes were preincubated for 20 min at 37°C. The reaction was then initiated with 80 mM dihydroorotate and quenched after 10 min of assay reaction by the addition of 1 ml 5% acetic acid. A color mix consisting of 2 ml of the diacetyl monoxime/antipyrine reagent was added and the assay mixture heated at 60 °C for 30-90min to generate a yellow color. The samples were briefly cooled and the absorbance measured at 466 nm.

3.5 Formation of the ATCase-DHOase Complex

The complex was prepared by mixing ATCase and DHOase in 1:1 mole-mole ratio followed by incubation on ice for 1 hr with gentle mixing.

3.6 Gel Filtration Chromatography

Proteins were eluted by size exclusion chromatography in decreasing order of size. The oligomeric structure of the individual enzymes and the possible interaction between them can be investigated using this technique. A 1.5 × 62 cm or 1.5 ×120 cm high resolution Sephacryl S-300 column was used in this study. Column beads were cleaned with 0.5M NaOH for 2hr then equilibrated with 50mM Tris/acetate buffer, pH 8.3. The flow rate of the column was 0.25 ml/min. Isolated ATCase or DHOase

(0.6 ml, of 2-3 mg/ml) or mixed (0.6 ml, of 2-3 mg/ml) in an equimolar ratio were loaded onto the column and allowed to flow through the column at a rate of 0.25 ml/min. The fractions were collected and analyzed by 12% SDS-PAGE gel electrophoresis and by enzyme assays.

3.7 Inhibition Studies

5-amino orotic acid, orotic acid, and 5-fluro orotic acid were used as inhibitors of the DHOase activity.

4. Results and Discussion

4.1 Expression of *B. Anthracis* Proteins

Plasmids encoding the *B. anthracis* proteins were expressed in *E. coli* BL21 (DE3) and the expressed proteins purified by affinity chromatography. Proteins were applied to a Ni^{2+} affinity chromatography resin and eluted with different imidazole concentrations. The fractions were analyzed for protein purity using SDS-PAGE. Purified *B. anthracis* ATCase and DHOase were typically obtained in the 200 mM imidazole/TN buffer (Figure 8). The purity of DHOase, 48 kDa, eluted with 200 mM imidazole, was judged greater than 90% by SDS-PAGE. The concentration of the purified protein, determined by the Lowry assay, ranged between 0.5 - 2.0 µg/µl.

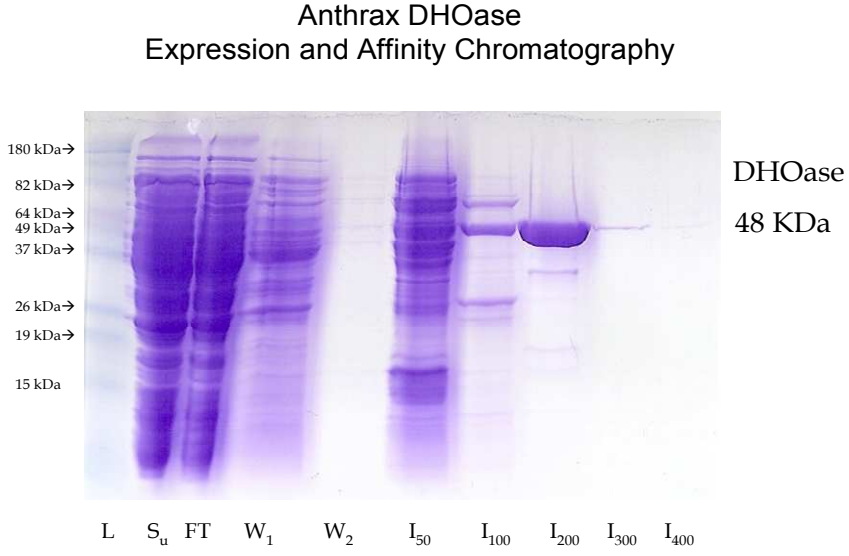

Figure 8: SDS-Page of *B. anthracis* DHOase expression and purification by Ni^{2+} affinity chromatography. Purified DHOase, 48 kDa, was eluted with 200 mM imidazole (I_{200}).

Purified *B. anthracis* ATCase (Figure 9), 36 kDa, was eluted with 200 mM imidazole. The concentration of the protein ranged between 0.5- 2.0 µg/µl as determined by the Lowry assay using BSA as the standard.

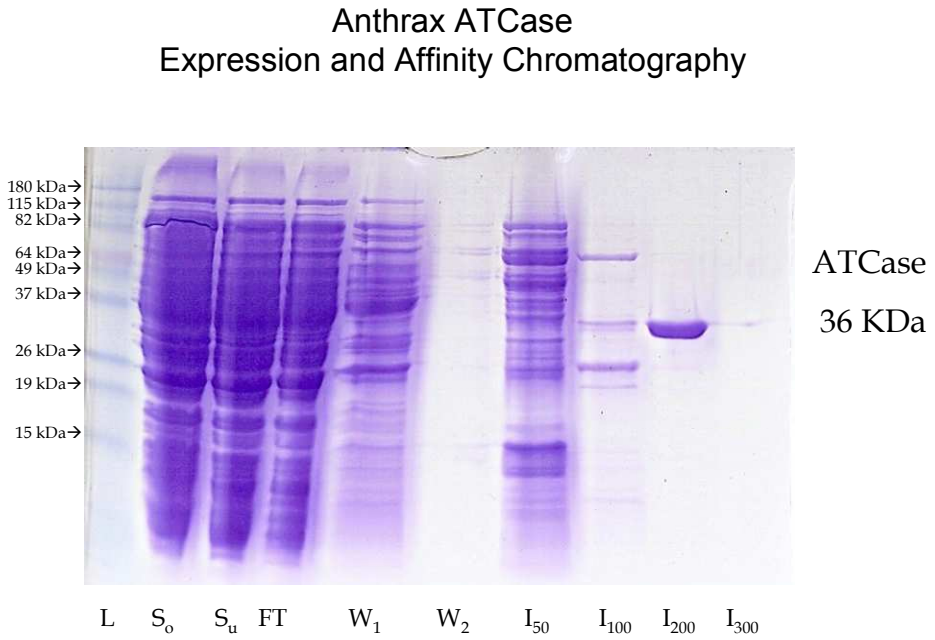

Figure 9: SDS-Page of *B. anthracis* ATCase expression and purification by Ni^{2+} affinity chromatography. Purified ATCase, 36 kDa, was eluted with 200 mM imidazole (I_{200}).

4.2 Enzymatic Assay of DHOase

The activity of DHOase (Figure 10) was determined by measuring the formation of carbamoyl aspartate at 37°C. The biosynthetic conversion of N-carbamoyl-L-aspartate to dihydro-L-orotate was also measured spectrophotometrically. The concentration of carbamoyl aspartate was calculated from a standard curve of known concentrations of carbamoyl aspartate. The 1-ml reaction mixture contained 50 mM Tris/acetate, pH 8.3, 1% glycerol, varying concentrations of dihydroorotate and 4.8 µg purified DHOase. The reaction mixture was pre-equilibrated for 20 min at 37°C and then

initiated by the addition of the substrate dihydroorotate or protein and quenched with 5% acetic acid after 20 min reaction time. A 2 ml color mix which contained a 1:2 (volume: volume) ratio of diacetyl monoxime and antipyrine was then added, and the tubes were incubated at 60°C for 30-90 min for yellow color development. The absorbance was measured at 466 nm. The linear increase in absorbance due to the formation of carbamoyl aspartate from dihydroorotate was followed. The equilibrium strongly favors dihydroorotate hydrolysis.

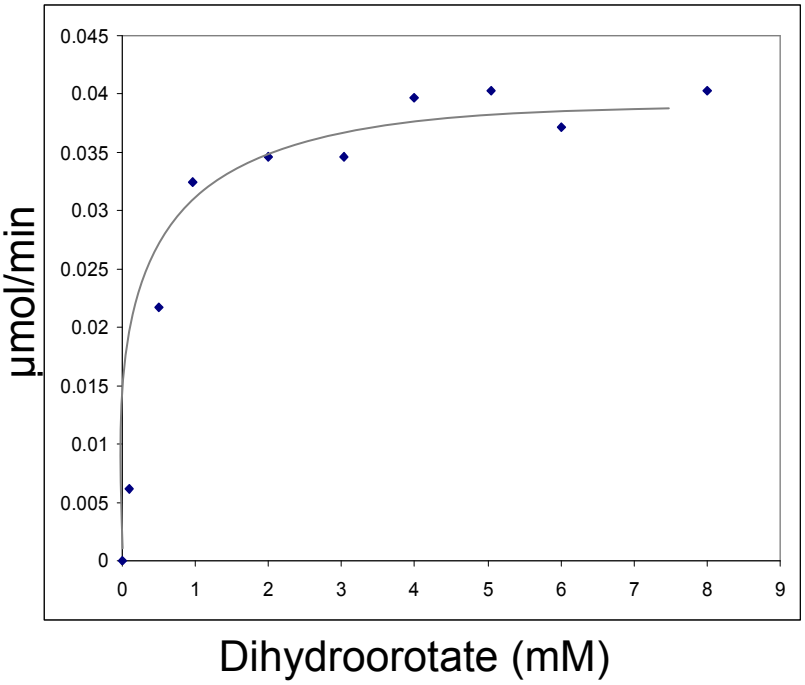

Figure 10: Dihydroorotate saturation curve of isolated *B. anthracis* DHOase.

4.3 Enzyme Assay of ATCase

The ATCase activity (Figure 11) was determined by measuring the formation of carbomyl aspartate from carbamoyl phosphate and aspartate. The 1 ml assay reaction consisted of 2 mM aspartate, 50 mM Tris/acetate, pH 8.3, 1% glycerol, 5 mM

carbamoyl phosphate, and 2 µg of purified protein. The reaction mixture was pre-warmed for 20 min at 37^{o}C and then initiated with either the protein or the substrate, carbamoyl phosphate. The reaction was allowed to proceed for 20 min and was then quenched with 1 ml 5% acetic acid. After the reaction was quenched, a 2 ml color mix consisting of a 1:2 (volume: volume) ratio of diacetylmonoxime and antipyrine was added and the mixture incubated at 60°C for 30-90 min for color development. The absorbance was then measured spectrophotometrically at 466 nm and the amount of carbamoyl aspartate formed calculated from the carbamoyl aspartate standard curve. The free Bacillus anthracis ATCase is active by itself. The increased information of carbamoyl aspartate from Carbamoyl phosphate was followed.

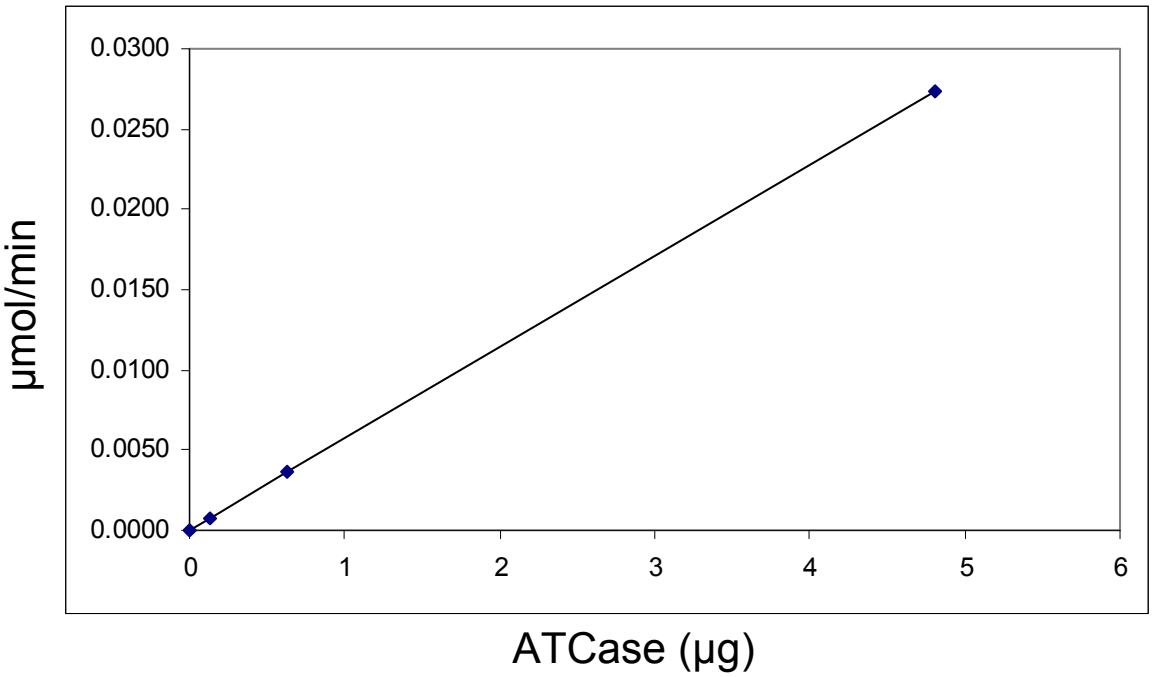

Figure 11: ATCase enzymatic assay of as a function of increasing concentrations of the protein.

4.4 Investigating Functional Interactions of the DHOase and ATCase Domains of *B. anthracis*

The isolated *B. anthracis* ATCase is catalytically active as is the isolated DHOase domain. Functional interactions among domains involved in pyrimidine biosynthesis have been documented in several systems that include that found in *Aquifex aeolicus.*[19] Therefore, to investigate whether the *B. anthracis* ATCase and DHOase domains may influence each other through functional interactions, assays of ATCase and DHOase were carried out in the presence of both proteins.

4.4.1: Effect of DHOase on the ATCase Activity: The ATCase and DHOase were mixed in 1:1 molar ratio and incubated on ice for 1hr. The activity of ATCase (Figure 12) in the absence or presence of DHOase was determined by measuring the formation of carbomyl aspartate from carbamoyl phosphate and aspartate as described above. The ATCase activity appears to be increased by nearly 2-fold in the presence of DHOase in a linear fashion.

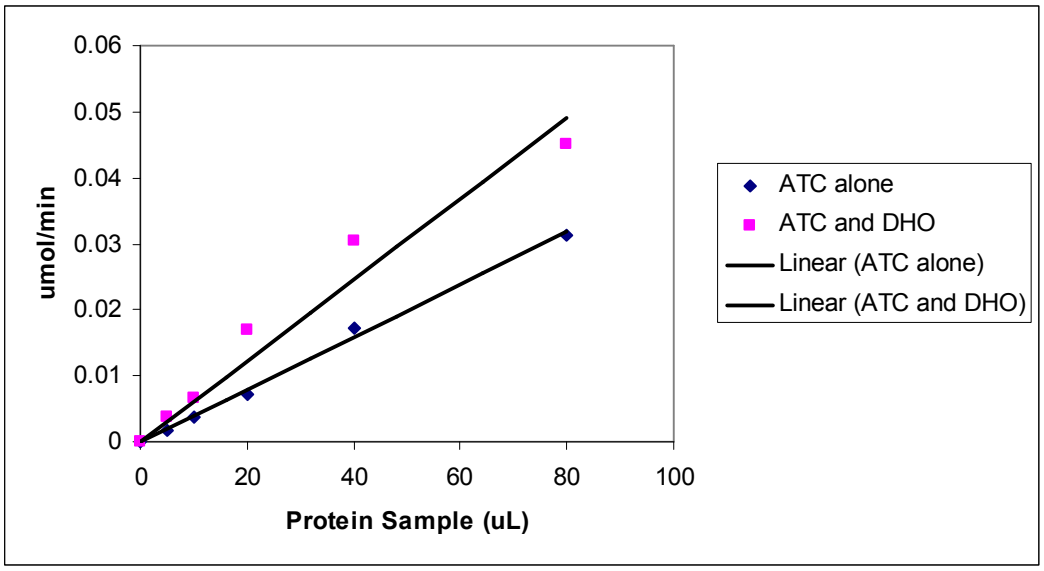

Figure 12: ATCase assay of the *B. anthracis* ATCase in the absence or in the presence of equimolar *B. anthracis* DHOase. The ATCase activity is increased in the presence of DHOase.

ATCase assays as a function of increasing carbamoyl phosphate (CP) concentrations were also carried out (Figure 13). The final concentrations of CP in the reaction tubes were 0 mM, 0.5 mM, 1 mM, 2 mM, 3 mM, 4 mM, and 5 mM. The reaction mixtures were allowed to pre-incubate for 20 min at 37°C and then initiated with 10µl of (0.72 µg/µl) ATCase protein and, in parallel reactions, with an equimolar concentration of ATCase and DHOase. The reactions were allowed to proceed for 20 min then quenched with 1ml 5% acetic acid, and the absorbance read at 466 nm, as described above.

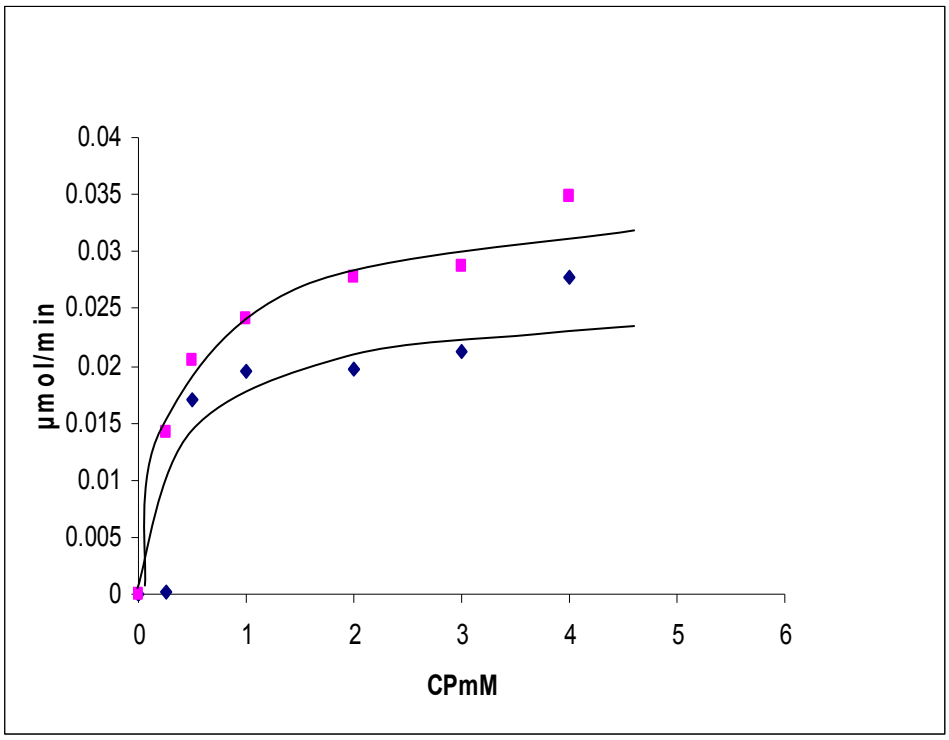

Figure 13: ATCase assay as a function of increasing carbamoyl phosphate (CP) concentrations of *B. anthracis* ATCase in the absence (◊) and in the presence of *B. anthracis* DHOase (□).

Addition of *B. anthracis* DHOase resulted in an apparent two-fold activation of *B. anthracis* ATCase, suggesting a functional linkage between the two enzymes.

4.4.2: *B. anthracis* DHOase Activates *B. anthracis* ATCase in a 1:1 mole/mole ratio: A fixed concentration of ATCase (0.86 µg/µl) was titrated with different concentrations of DHOase (0.60 µg/µl) (DHOase/ATCase: 1:10, 5:10, 10:10, 20:10, 40:10, 60:10, 100:10) in order to find the amount of DHOase needed to activate the ATCase. The enzyme activity at different protein ratios were assayed as well as

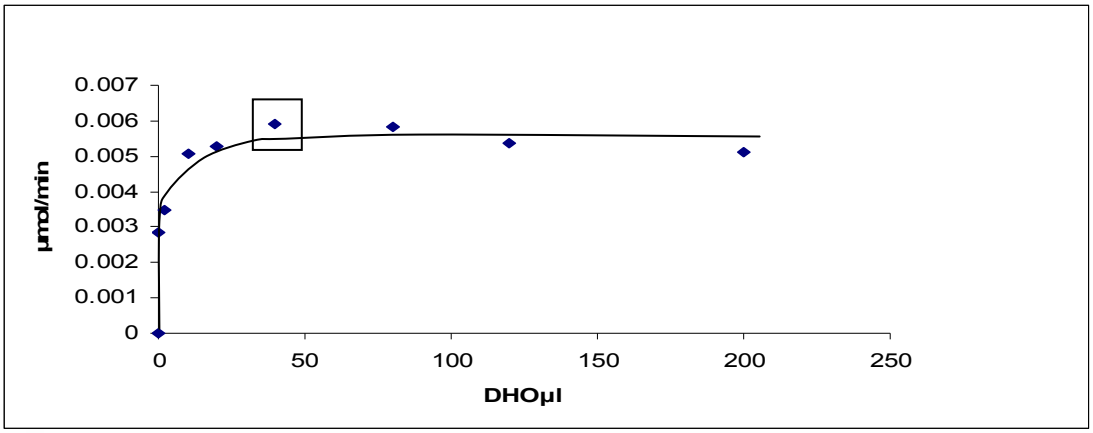

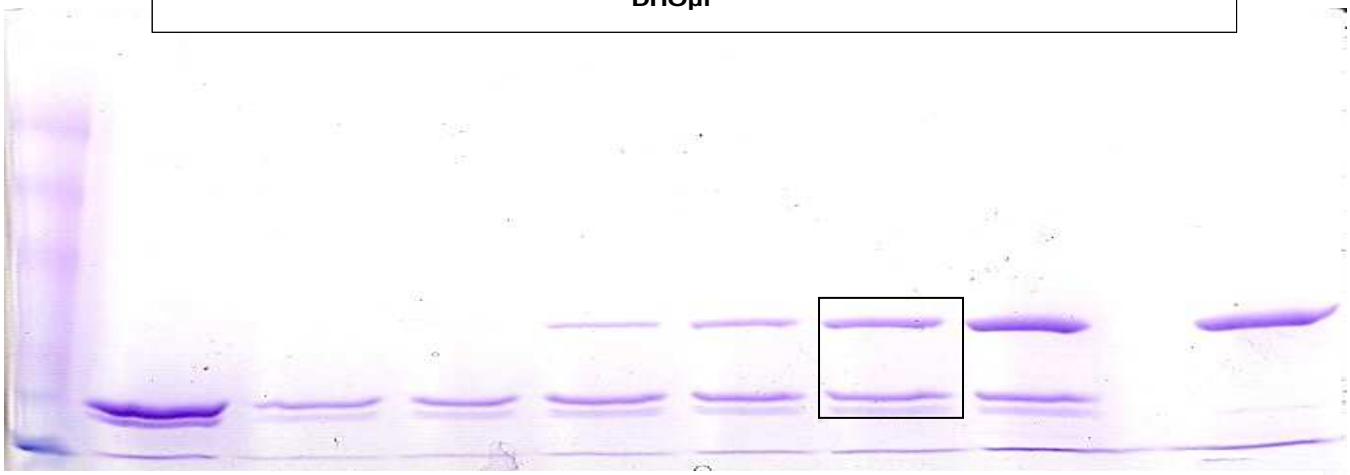

ATC (nmol)	5	1	1	1	1	1	1	0
DHO (nmol)	0	0	0.05	0.25	0.5	1	4	5

Figure 14: SDS-PAGE gel and ATCase enzyme assay with a fixed *B. anthracis* ATCase concentration and increasing concentrations of *B. anthracis* DHOase. 1 mole of the DHOase was required to achieve maximal activation of 1 mole of ATCase. The points on the assay and gel corresponding to an equimolar concentration of both proteins are boxed.

visualized by SDS-PAGE (Figure 14). The ATCase activity increases with increasing concentrations of DHOase and stabilized until the DHOase and ATCase concentrations were equimolar. Addition of increasing molar concentrations of DHOase did not result in further activation.

4.5 *A. aeolicus* DHOase Weakly Activates *B. anthracis* ATCase

The finding that the *B. anthracis* ATCase is optimally activated by equimolar concentrations of *B. anthracis* DHOase suggests a functional interaction between the two proteins. To investigate the specificity of this interaction, *A. aeolicus* DHOase, which has a high sequence similarity to *B. anthracis* DHOase, was added at various molar ratios (Figure 15) to *B. anthracis* ATCase to examine its ability to activate the enzyme. *A. aeolicus* DHOase was able to activate the ATCase from *B. anthracis* but much more weakly than the DHOase from *B. anthracis*. While it took 1 mole of *B. anthracis* DHOase to fully activate the ATCase (Figure 14), the enzyme was activated by only 50% at 25 moles of *A. aeolicus* DHOase per 1 mole of ATCase. Moreover, full activation of *B. anthracis* ATCase required 50 moles of *A. aeolicus* DHOase. These results suggest that optimal activation of *B. anthracis* ATCase is achieved by specific interactions with *B. anthracis* DHOase. These interactions appear not to be conserved in the *A. aeolicus* enzyme.

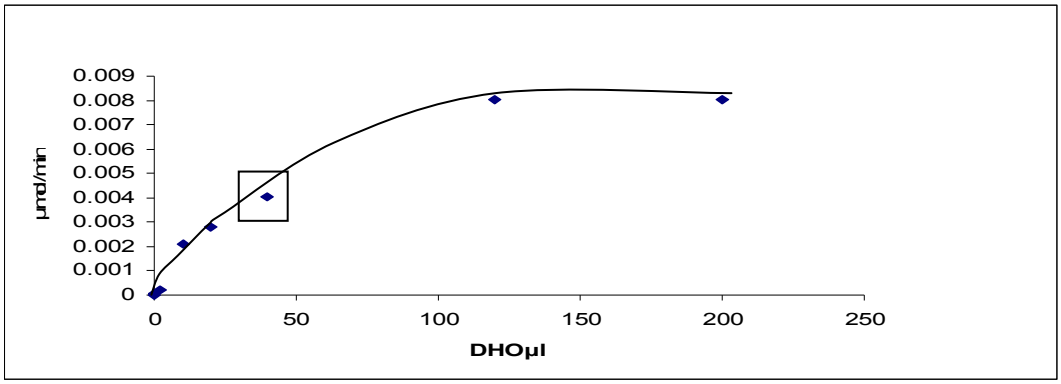

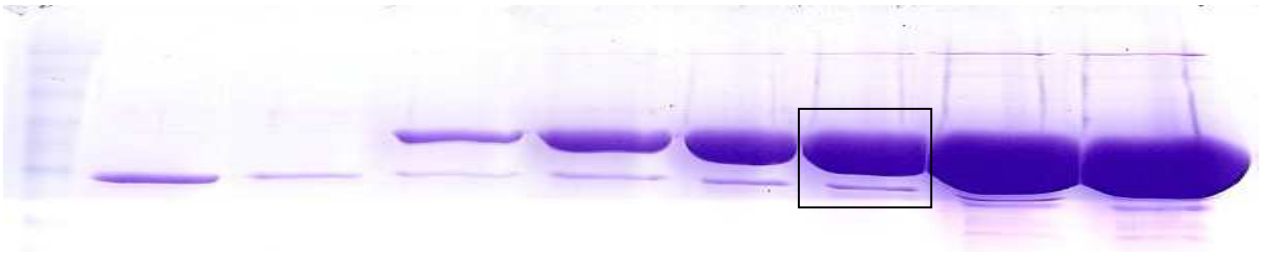

DHO (nmol)	0	0	4	10	15	25	50	50
ATC (nmol)	5	1	1	1	1	1	1	0

Figure 15: ATCase activity and SDSPAGE of a fixed concentration of *B. anthracis* ATCase and different concentrations of *A. aeolicus* DHOase. *A. aeolicus* DHOase weakly activates *B. anthracis* ATCase as compared to *B. anthracis* DHOase. The boxed lane on the SDS-gel corresponds to the boxed point on the assay curve.

4.5.1 Effect of ATCase on DHOase: The DHOase activity of *B. anthracis* DHOase was assayed (Figure 16) in the absence or presence of equimolar *B. anthracis* ATCase to investigate putative functional interactions between the two domains. The isolated *B. anthracis* DHOase was found to be catalytically active in the absence of *B. anthracis* ATCase, a situation that differs remarkably from that of *A. aeolicus*, in which the isolated DHOase is only active in the presence of the *A. aeolicus* ATCase domain.[19] Interestingly, the *B. anthracis* DHOase does not appear to be affected by the presence of *B. anthracis* ATCase under these conditions.

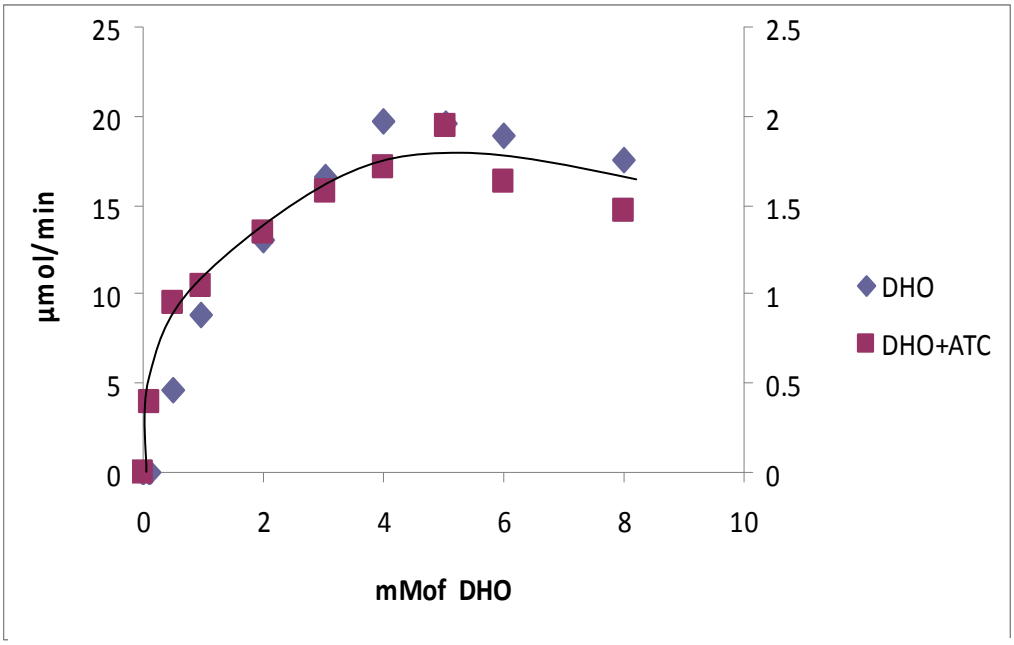

Figure 16: A dihydroorotate saturation curve of *B. anthracis* DHOase in the absence or presence of equimolar *B. anthracis* ATCase. No stimulation of activity is apparent in the presence of *B. anthracis* ATCase under these conditions.

4.6: B. anthracis ATCase cannot activate *A. aeolicus* DHOase

The ATCase from *B. anthracis* shares a high sequence similarity with the ATCase from *A. aeolicus*. The isolated *A. aeolicus* DHOase is completely inactive and needs associations with the *A. aeolicus* ATCase to become catalytically active. To investigate the specificity of the interactions in *B. anthracis*, we wanted to examine whether the *A. aeolicus* DHOase can be activated by the ATCase from *B. anthracis*.

A dihydroorotate saturation curve was carried out (Figure 17) to assay for the activity of isolated *A. aeolicus* DHOase in the absence or presence of stoichiometric amounts of *A. aeolicus* ATCase and *B. anthracis* ATCase.

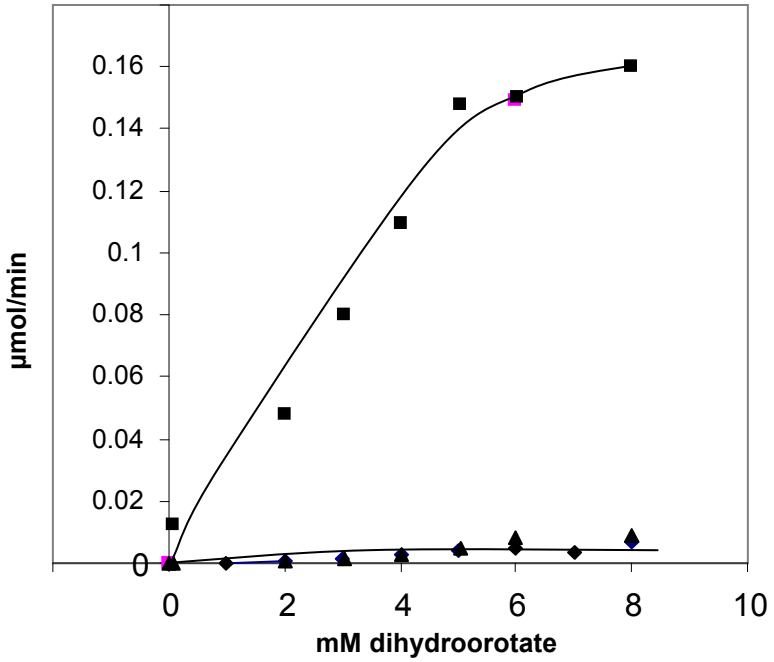

Figure 17: DHOase assay as a function of increasing dihydroorotate concentration of *A. aeolicus* DHOase alone (♦), in the presence of *A. aeolicus* ATCase (■) or in the presence of *B. anthracis* ATCase (▲).

As expected and in accord with previous findings,[19] isolated *A. aeolicus* DHOase assayed alone showed no catalytic activity unless in the presence of *A. aeolicus* ATCase. Interestingly, *B. anthracis* ATCase was not able to activate the *A. aeolicus* DHOase despite its high sequence identity with the *A. aeolicus* ATCase.

These results clearly show that *B. Anthracis* ATCase is activated by stoichiometric amounts of *B. anthracis* DHOase, while the DHOase is not activated by ATCase under these assay conditions. The reverse is observed in the *A. aeolicus* system. The ATCase domain is not activated by the DHOase, and the isolated *A. aeolicus* DHOase is completely inactive in the absence of ATCase despite the

presence of all the active site residues and metal binding residues needed for catalysis.

These interactions appear to be highly specific. As mentioned above, the *A. aeolicus* DHOase has a high sequence similarity with that of *B. Anthracis* DHOase with a percent sequence identity of 43%. However, despite the high sequence similarity, *A. aeolicus* DHOase only weakly activated the ATCase from *B. anthracis*. Moreover, despite the high sequence similarity of the ATCase from *A. aeolicus* and *B. anthracis*, the *B. anthracis* ATCase failed to activate the *A. aeolicus* DHOase.

4.7 Inhibitor Assays

An important objective of studying the *B. anthracis* pyrimidine enzymes is the development of drugs that can selectively inhibit the bacterial pathway with minimum or no effect on the mammalian pathway. The purified DHOase from *B. anthracis* was assayed with known inhibitors of DHOases from other organisms: 5-amino orotic acid, orotic acid, and 5-fluroorotic acid (Figure 18). The assays show that orotate was able to inhibit *B. anthracis* DHOase at nanomolar concentrations. However, as orotate is the product of the next enzyme in the pathway, dihydroorotate dehydrogenase (Figure 2), modified compounds that resemble orotate need to be designed to more selectively inhibit the dihydroorotase domain, a domain clearly found to be indispensible for the *B. anthracis* bacterial growth.

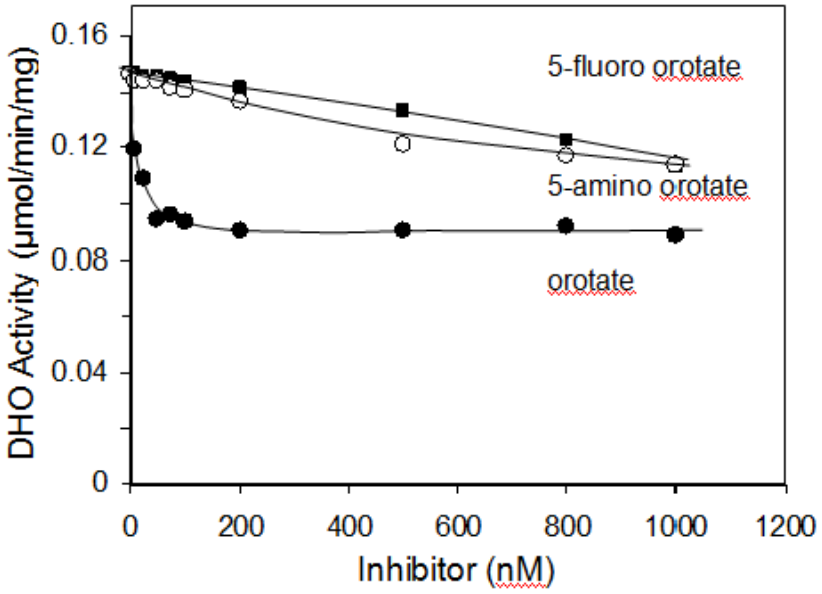

Figure 18: Inhibition assays of B. anthracis DHOase

4.8 Gel Filtration Chromatography

B. anthracis ATCase, 0.6 ml (0.5 mg) was applied onto an S-300 Sephacryl gel filtration column, and the protein was eluted with a buffer consisting of 50 mM Tris/acetate, pH 8.0, 200 mM sodium chloride, and 10% glycerol. Fractions (1 ml) each were collected and analyzed by SDS-PAGE. Fractions corresponding to the peak (Figure 19) were tested for enzymatic activity. The peak fractions, lanes 4-6,

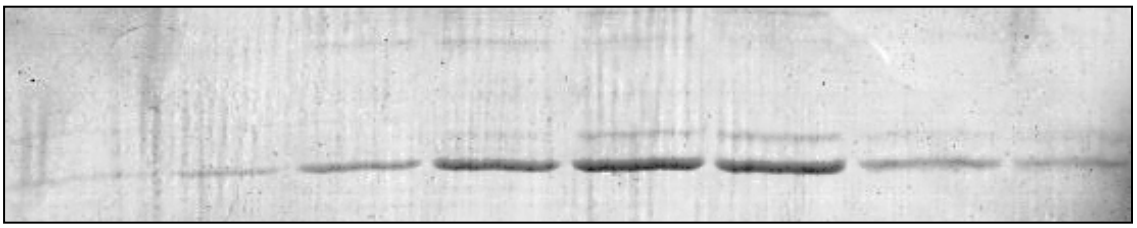

B. anthracis ATCase is a trimer

Lane: 1 2 3 4 5 6 7 8

Figure 19: S-300 gel filtration chromatography fractions of *B. anthracis* ATCase

showed the highest ATCase activity.

B. anthracis DHOase, 0.6 ml (0.75 mg) was applied to a S-300 Sephacryl gel filtration column and eluted with a buffer consisting of 50 mM Tris/acetate, pH 8.0, 200 mM sodium chloride, and 10% glycerol (Figure 20). Fractions corresponding to the peak (Figure 20) were tested for enzymatic activity. The peak fractions, lanes 2-6, showed the highest DHOase activity.

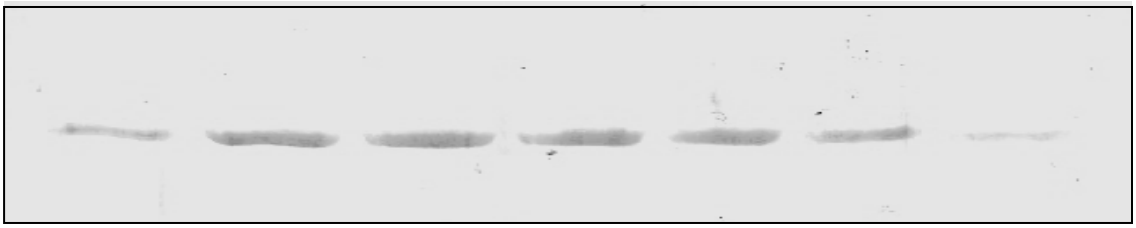

B. anthracis DHOase is a homodimer

Lane: 1 2 3 4 5 6 7

Figure 20: S-300 gel filtration chromatography fractions of *B. anthracis* DHOase

A stoichiometric mixture of ATCase and DHOase (0.6 ml) was preincubated at room temperature for 20 min and then loaded onto the S-300 gel filtration column. The proteins were eluted in a buffer consisting of 50 mM Tris/acetate, pH 8.0, 200 mM sodium chloride, and 10% glycerol. The fractions were then analyzed using SDS-PAGE (Figure 21). Fractions corresponding to the peak (4-7) had both ATCase and DHOase activities. The two proteins eluted in the same fractions, suggesting formation of a complex most likely to be a dodecamer consisting of 2 ATCase trimers and 3 DHOase dimers. This complex likely resembles that found in *A. aeolicus*.

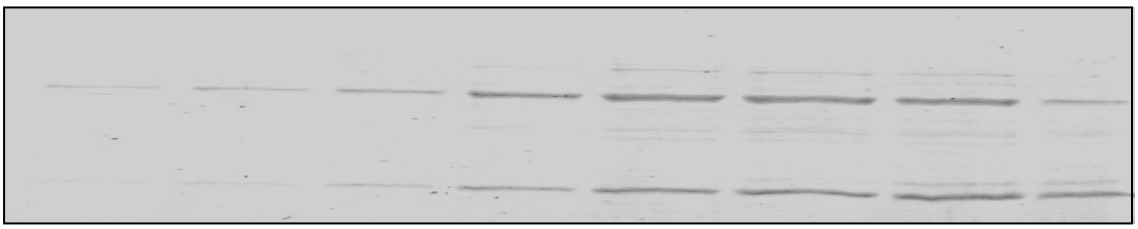

B. anthracis ATCase and DHOase is likely a dodecamer

Lane: 1 2 3 4 5 6 7 8

Figure 21: S-300 gel filtration chromatography fractions of *B. anthracis* DHOase and ATCase

5. Summary

1) S-300 Sephacryl gel filtration chromatography suggests that a complex, likely a dodecamer, is formed between *B. anthracis* ATCase and DHOase.
2) Enzyme assays showed that *B. anthracis* ATCase and *B. anthracis* DHOase are active individually and that they do not depend on each other for catalytic activity.
3) In a stoichiometric complex between *B. anthracis* ATCase and *B. anthracis* DHOase, DHOase appears to activate ATCase by nearly twofold, while ATCase does not appear to further activate the DHOase.
4) The opposite effect is found in the analogous *A. aeolicus* system where the DHOase is completely inactive unless associated with the ATCase domain and where the ATCase activity is not stimulated by DHOase. This is despite the high sequence identity between the two enzymes in the two systems.
5) *A. aeolicus* DHOase can activate *B. anthracis* ATCase, albeit very weakly. Much higher molar ratios are required for the observed effects. These results support the specificity of the interactions between the enzymes in the same system.
6) Orotate inhibits the *B. anthracis* DHOase at nanomolar levels. This finding sets the stage for the development of drugs that can mimic orotate and selectively inhibit the *B. anthracis* DHOase.

6. Future Studies

Determining the three dimensional structure of the *B. anthracis* DHOase-ATCase complex will provide invaluable information of the overall structure and a close-up view of the active sites. The information obtained will shed light on the specific functional interactions between the two proteins and aid in the design of specific inhibitors that will likely result in the development of new therapeutic approaches to infections resulting from the bacteria, *B. anthracis*.

7. References

1) Shalaka Samant, Hyunwoo Lee, Mahmood Ghassemi, Juan Chen, James L. Cook, Alexander S. Mankin, Alexander A. Neyfakh; Nucleotide Biosynthesis Is Critical for Growth of Bacteria in Human Blood; *PLoS Pathog* 4(2):, **2008,** e37. doi:10.1371/journal.ppat.0040037.
2) Mylotte JM, Tayara A; Blood cultures: clinical aspects and controversies; *Eur J Clin Microbiol Infect Dis* 19: 157–163, **2000**.
3) Lyons CR, Lovchik J, Hutt J, Lipscomb MF, Wang E, et al., Murine model of pulmonary anthrax: kinetics of dissemination, histopathology, and mouse strain susceptibility. *Infect Immun* 72: 4801–4809, **2004**.
4) Smith LK, Gomez MJ, Shatalin KY, Lee H, Neyfakh AA, Monitoring of Gene Knockouts: genome-wide profiling of conditionally essential genes. *Genome Biol* 8: R87, **2007**.
5) Thoden JB, Phillips GN Jr., Neal TM, Raushel FM, Holden HM; Molecular structure of dihydroorotase: a paradigm for catalysis through the use of a binuclear metal center. *Biochemistry* 40: 6989–6997, **2001**.
6) Serkan S, Selcen O, Serhan S, Anthrax – an overview, *Med Sci Monit*; 9(11): RA276-283, **2003**.
7) Evans DR, Guy HI, Mammalian pyrimidine biosynthesis: Fresh insights into an ancient pathway J Biol Chem. 279: 33035-33038, **2004**.
8) Grayson DR, Evans DR. The isolation and characterization of the aspartate transcarbamylase domain of the multifunctional protein, CAD. *J Biol Chem.* 1983 Apr 10; **258**(7):4123–4129.

9) Maley JA, Davidson JN. The aspartate transcarbamylase domain of a mammalian multifunctional protein expressed as an independent enzyme in Escherichia coli. *Mol Gen Genet.* 1988 Aug;213(2-3):278–284

10) Scully, J. L., and Evans, D. R.; Comparative modeling of mammalian aspartate transcarbamylase *Proteins* 9, 191–206, **1991**.

11) Qiu, Y. and J.N. Davidson. Substitutions in the aspartate transcarbamoylase domain of hamster CAD disrupt oligomeric structure. Proc. Natl. Acad. Sci. USA 97: 97-102, **2000**.

12) Thoden, J. B., Phillips, G. N., Jr., Neal, T. M., Raushel, F. M., and Holden, H. M.; "Molecular Structure of Dihydroorotase: A Paradigm for Catalysis Through the Use of a Binuclear Metal Center"*Biochemistry* 40, 6989–6997, **2001**.

13) Fields, C., Brichta, D., Shephardson, M., Farinha, M., and O'Donovan, G.; *Paths Pyrimidines* 7, 49–63, **1999**.

14) Kelly, R. E., Mally, M. I., and Evans, D. R.; *J. Biol. Chem.* 261, 6073–6083, **1986**.

15) Musmanno, L. A., Maley, J. A., and Davidson, J. N.; *Gene* (*Amst*.) 99, 211–216, **1991**.

16) Williams, N. K., Peide, Y., Seymour, K. K., Ralston, G. B., and Christopherson, R. I.; *Protein Eng.* 6, 333–340, **1993**.

17) Zimmermann, B. H., and Evans, D. R. (1993) *Biochemistry* 32, 1519–1527, **1993**.

18) Structure of dihydroorotase from Bacillus anthracis at 2.6A°resolution*;* Shahila Mehboob, Debbie C.Mulhearn, Kent Truong,Michael E. Johnson and Bernard D. Santarsiero, *Acta Cryst.* **2010**. F66, 1432–1435.

19) Ahuja, A., Purcarea, C., Ebert, R., Guy, H., and Evans, D.; *Aquifex aeolicus* dihydroorotase: Association with aspartate transcarbamoylase switches on catalytic activity, *J. Biol. Chem. 279*, 53136-53144, **2004**.